

## Adhesion and composite micro-hardness of DLC and Si-DLC films deposited on nitrile rubber

Kevin McDonnell

*Surface and Coatings Technology*

### Cite this paper

Downloaded from [Academia.edu](#) 

[Get the citation in MLA, APA, or Chicago styles](#)

### Related papers

[Download a PDF Pack](#) of the best related papers 



[Characteristics and tribological performance of DLC and Si-DLC films deposited on nitrile rubber](#)  
Kevin McDonnell

[Microstructure and Mechanical Properties of Ti/AlTiN/Ti-Diamondlike Carbon Composite Coatings on...](#)  
Alex A Volinsky

[AlTiN Layer Effect on Mechanical Properties of Ti-doped Diamond-like Carbon Composite Coatings, X...](#)  
Alex A Volinsky



## Adhesion and composite micro-hardness of DLC and Si-DLC films deposited on nitrile rubber

M. Lubwama <sup>a,\*</sup>, B. Corcoran <sup>a</sup>, K. Sayers <sup>b</sup>, J.B. Kirabira <sup>c</sup>, A. Sebbit <sup>c</sup>, K.A. McDonnell <sup>d</sup>, D. Dowling <sup>d</sup>

<sup>a</sup> School of Mechanical and Manufacturing Engineering, Dublin City University, Dublin 9, Ireland

<sup>b</sup> Department of Mechanical Engineering, Dundalk Institute of Technology, Dundalk, Ireland

<sup>c</sup> Department of Mechanical Engineering, Makerere University, P.O. BOX 7062, Kampala, Uganda

<sup>d</sup> School of Mechanical and Materials Engineering, University College Dublin, Dublin 4, Ireland

### ARTICLE INFO

#### Article history:

Received 4 April 2012

Accepted in revised form 20 May 2012

Available online 26 May 2012

#### Keywords:

Adhesion

Closed field unbalanced magnetron

sputtering ion plating

DLC

Micro-hardness

Si-DLC

Tribology

### ABSTRACT

Thin films of hydrogenated diamond-like carbon (DLC) and silicon (Si) doped diamond-like carbon (Si-DLC) have been deposited on acrylonitrile butadiene rubber (NBR) using a closed field unbalanced magnetron sputtering ion plating system. A sputter cleaning process was integrated into the deposition process so as to reduce the likelihood of re-contamination between the cleaning and deposition stages. The deposited coatings showed excellent adherence with an adhesion rating of 4 A for films with a Si-C interlayer. The composite micro-hardness was highest for DLC films at 15.5 GPa for indentation load of 147.1 mN using a Vickers micro-hardness tester. Tribological tests undertaken under normal load of 5 N using a pin-on-disc tribometer for all of the samples of DLC and Si-DLC films, with and without Si-C interlayer, show a friction increase between 0.25 and 0.4 to between 0.45 and 0.6. This friction increase has been related to the micro-hardness of the films.

© 2012 Elsevier B.V. All rights reserved.

### 1. Introduction

A potential application for DLC and doped DLC coatings is to enhance the performance of nitrile rubber (NBR) piston seals in handpumps for rural water supply in developing countries by reducing their wear rates. Such seals experience a combination of dry and wet sliding and prolonged aqueous immersion depending on the height of the local water table and operating regime. During wet sliding and prolonged aqueous immersion suspended solids accelerate the wear rate of these NBR piston seals. As a consequence the duty cycle for pump seals is heavy resulting in few functional handpumps shortly after installation.

Diamond-like carbon (DLC) coatings are commonly used to increase wear resistance of materials in industry. Recently, much attention has been given to the application of DLC and doped DLC coatings onto rubber substrates [1–6]. In all of these studies it has been shown that the tribological properties of DLC coatings on rubber are excellent as they reduce the coefficient of friction and wear rates when compared to uncoated substrates. For good performance, DLC and DLC based coatings deposited on rubbers should have strong adhesion to rubber substrates, be sufficiently flexible to adapt to the large strain of rubbers under load and have good wear resistance and low friction

[6]. The elemental composition, surface roughness profiles and film thickness of DLC and Si-DLC films with and without Si-C interlayers were discussed in our previous paper [7].

Adhesion and micro-hardness are two important characteristics for assessing the properties and performance of thin films [8]. The adhesion of DLC on polymer substrates has been researched by other groups and evaluated by the scratch test [9], adhesive tape test [10], and resistance to thermal cycling [11]. Adhesion improvement has been achieved by pre-treatment of the substrate surface and varying of the coating deposition conditions [12]. Bui et al. [6] observed that pre-deposition plasma treatment of rubber substrate improved the adhesion of hydrogenated DLC thin films onto the rubber substrate after performing stretch tests with a tensile stage inside a scanning electron microscope (SEM). However, for DLC and DLC based coatings, deposited on rubber, relatively little has been published regarding the adhesion of the DLC coating and the relation between composite micro-hardness and tribological behaviour.

In this study DLC and Si-DLC with and without Si-C interlayers are deposited on nitrile rubber using a closed field unbalanced magnetron sputtering ion plating system. The adhesion between the films and the substrate was determined using the peel test method by applying an X-cut and observation using optical microscopy [13,14]. The composite micro-hardness was determined using a Leitz mini-load hardness tester. The composite micro-hardness of the films on the NBR substrates was related to the tribological behaviour of the films at a normal load of 5 N under dry sliding using a pin-on-disc tribometer.

\* Corresponding author. Tel.: +353 85 229 5129; fax: +353 1 700 5345.

E-mail address: [michael.lubwama2@mail.dcu.ie](mailto:michael.lubwama2@mail.dcu.ie) (M. Lubwama).

## 2. Experimental

Black acrylonitrile butadiene rubber (NBR) sheet of 3 mm thickness with Shore A hardness of  $70 \pm 5$  was used as the substrate in this study. Plasma etching pre-treatment of rubber substrates and deposition of DLC films were carried out using a closed field unbalanced magnetron sputtering ion plating system, which consisted of four magnetrons evenly distributed around the chamber. Fig. 1 shows a cross-section of a closed field unbalanced magnetron sputtering chamber. Two opposite magnetrons were used as carbon targets and one magnetron was used as the Si target. The fourth magnetron in the system was not used during the deposition process. Three pieces of NBR rubber with dimensions 100 mm by 100 mm by 3 mm thickness were mounted onto a holder in the centre of the system facing outwards towards the target. The sample holder was rotated at a speed of 5 rpm. NBR substrates were etched in 150 kHz pulsed-dc Ar plasma for 10 min at a bias voltage of  $-200$  V. The deposition process followed immediately after the plasma etching pre-treatment so as to reduce the likelihood of re-contamination between the cleaning and deposition process [15]. The total deposition time for DLC was 60 min. This process was repeated for all samples including the Silicon doped DLC (Si-DLC) samples. The gas flow rate was set at  $\text{Ar}/\text{C}_4\text{H}_{10} = 12$  sccm/8 sccm and the NBR substrates were biased with pulsed DC (150 kHz with a pulse off time of 150 ns) at a substrate bias of  $-30$  V all of which were held constant. In order to achieve the dopant of Si in Si-DLC, a current of 0.5 A was supplied to the Si target during the deposition. The Si-C interlayer was obtained by supplying a current of 1 A to the Si target and 1 A to the pure C target. The Si-C interlayer deposition time was 35 min and the subsequent time for DLC deposition was 40 min. Fig. 2 shows the process design for DLC and Si-DLC films deposited on NBR substrates.

Raman spectra were acquired to investigate the chemical bonding of these films by using a LabRAM Horiba Jobin Yvon spectrometer equipped with a CCD detector and an Ar laser (488 nm) at 8 mW. All of the measurements were recorded for the wavelength range of 500 to 2000  $\text{cm}^{-1}$  using the same conditions (5 s of integration time and 5 accumulations) using a 100 $\times$  magnification objective and a 200  $\mu\text{m}$  pinhole.

For hardness measurements the DLC and Si-DLC films, with and without Si-C interlayers, were deposited on a silicon wafer under similar process conditions as deposition on the NBR substrate to a thickness of about 1  $\mu\text{m}$ . Such an approach has been used by Bui et al. [3], who determined the hardness of Ti-DLC deposited on Si wafer instead of HNBR rubber, despite the fact that the structure of coatings deposited on rubber is rather different from that on Si wafer. This approach is used as reference, due to the difficulty in precise measurement of hardness of coatings deposited on rubber. Under the same deposition conditions, the hardness of the coating on rubber might be lower than that on Si due to release of residual stresses, but the trend of hardness results is expected to be the same [3]. Film micro-hardness was

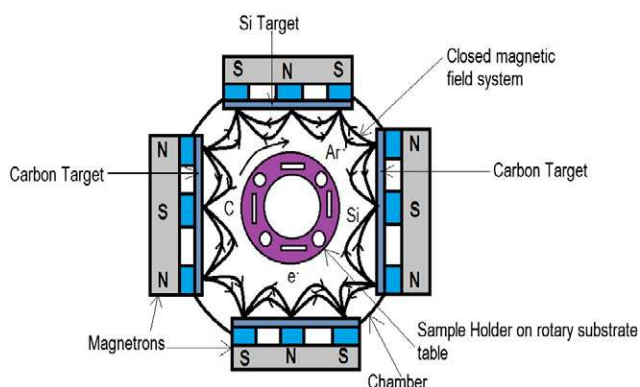


Fig. 1. Cross-section of closed field unbalanced magnetron sputtering chamber.

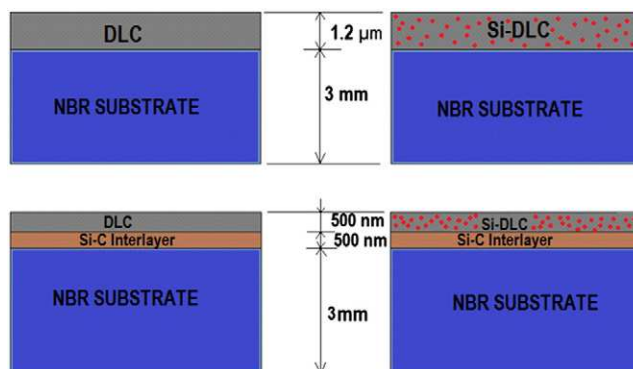


Fig. 2. Process design for DLC and Si-DLC films deposited on NBR substrate.

evaluated by Vickers micro-hardness tests (Leitz mini-load hardness tester, Serial No. 88134). After calibrating the system using a standard block, Vickers micro-hardness tests were performed with applied loads of 147.1 mN, 490.3 mN and 980 mN. Vickers micro-hardness (Hv) was determined by measuring the lengths of the diagonals of each indent at a magnification of 50 $\times$  using an optical microscope system within the micro-hardness tester.

Adhesion of the films on NBR substrates was evaluated using the X-cut method. The 'X' mark on the film had an angle of 30° between incisions [13,16]. A cellophane pressure sensitive adhesive tape (Scotch® with adhesion to steel of 49 N/100 mm width) was carefully adhered to the surface of the film at room temperature. After adhesion for 1–2 min, the tape was pulled off rapidly (not jerked) back upon itself at as close to an angle of 180° as possible. The peeling of the film at the X-cut area was observed by optical microscopy (EMZ-5TR Meiji Microscope with IC Capture software and Camera). Table 1 presents the film adhesion ratings for the adhesion tape test according to ASTM D3359-97 [16].

The tribological performance was evaluated at room temperature using a pin-on-disc (POD 2) tribometer. The counterpart was a standard Ø5 mm commercial WC-Co ball. The sliding speed was maintained at a linear speed of 10 cm/s at correlative test track diameters of 6 and 10 mm. Tribo-tests were carried out for normal load of 5 N.

## 3. Results and discussion

### 3.1. Raman spectroscopy

The chemical bonding of DLC and Si-DLC films has been studied by means of Raman spectroscopy using a 488 nm excitation wavelength. Fig. 3 represents typical full spectra for samples of DLC and Si-DLC coatings, showing the prominent G and smaller underlying D peaks (centred approximately 1580  $\text{cm}^{-1}$  and 1350  $\text{cm}^{-1}$  respectively). The ratio of the intensities of the D peak,  $I_D$ , and the G peak,  $I_G$ , the full width half maximum (FWHM) and peak heights were quantified after fitting the individual G and D peaks from the spectra with double

Table 1  
Levels of film adhesion ratings according to ASTM D3359-97.

Adhesion Level	Comment
5A	No peeling or removal occurs at all (absence of peeling)
4A	Trace peeling or removal occurs along incisions (no peeling occurs at the intersect and little peeling observed at the X-cut)
3A	Jagged removal along incisions occurs up to 1/16 in. (1.6 mm) on either side of the intersect of the X-cut
2A	Jagged removal along incisions occurs up to 1/8 in. (3.2 mm) in either direction from the intersect of the X-cut
1A	Most of the X-cut area peeled off with the adhesive tape
0A	Removal beyond the X-cut area occurs

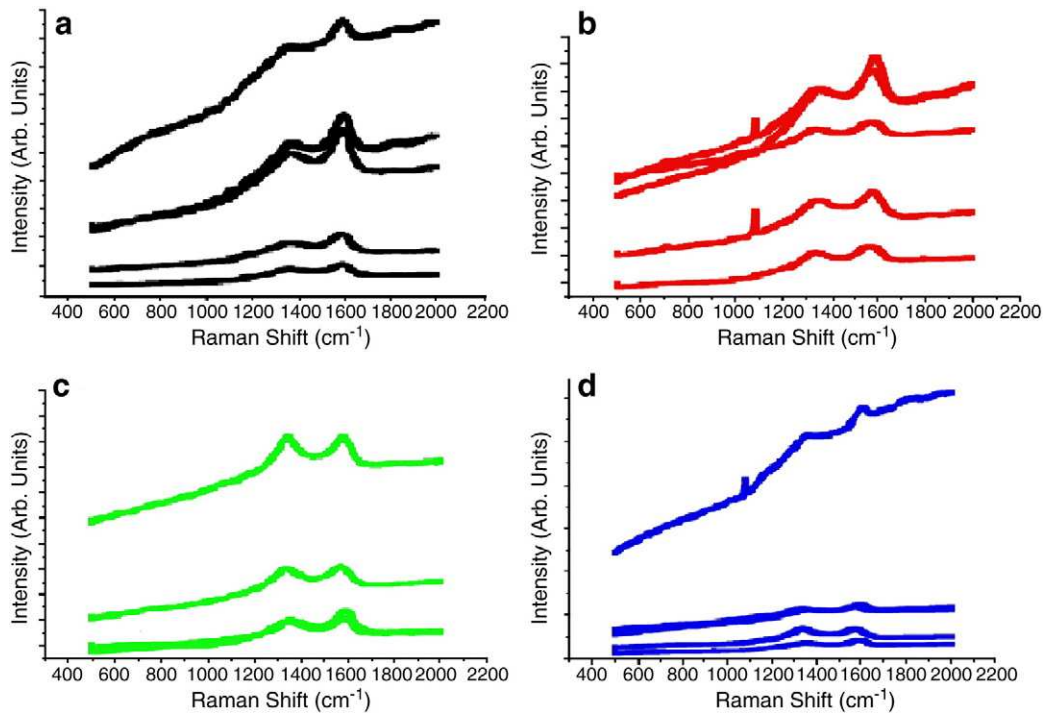


Fig. 3. Raman spectra for DLC (a), Si-DLC (b), DLC with Si-C interlayer (c), and Si-DLC with Si-C interlayer (d) films deposited on NBR substrate.

Gaussian functions. A sharply peaked band at around  $1060\text{ cm}^{-1}$ , the so called T peak, is observed for Si-DLC and Si-DLC with Si-C interlayer deposited on NBR substrate [17]. The T peak signifies an increase in Raman scattering contributions from  $\text{sp}^3$  sites due to vibration in C–C  $\text{sp}^3$  bonds [17]. The T peak was observed for the Si-DLC film and the Si-DLC film with Si-C interlayer. No such peak was observed for Raman spectra for DLC film and DLC film with Si-C interlayer. This may imply that the Si dopant in the DLC film, and not the Si-C interlayer, is the contributing factor for its presence in the Raman spectra. Such an explanation is supported by Paik [18] who observed a sharp Si-related peak at  $950\text{ cm}^{-1}$  for DLC films (20 nm thick) deposited on Si wafer by magnetron sputter-type negative ion source method.

The FWHM of the G peak and the  $I_D/I_G$  ratio for the DLC and Si-DLC films is depicted in Fig. 4. It is observed that the FWHM of the G peak is lower for DLC and Si-DLC films with Si-C interlayer, which suggests that the graphitic clusters were unstrained [19]. FWHM of the G peak measures the bond length and bond disorder in  $\text{sp}^2$  clusters, which have close relations with the stress felt by the clusters. With

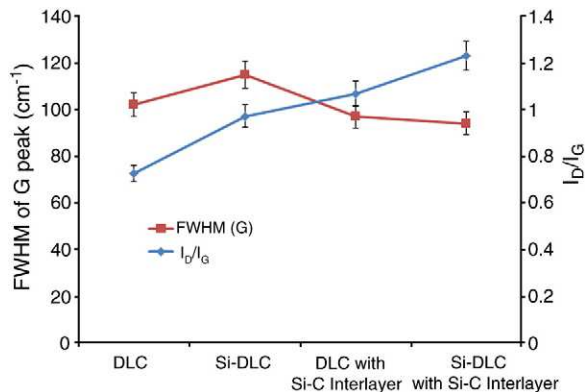


Fig. 4. FWHM of the G peak and  $I_D/I_G$  ratio for DLC and Si-DLC films without and with Si-C interlayer.

increasing  $\text{sp}^3$  content,  $\text{sp}^2$  clusters with  $\text{sp}^3$  networks become smaller and more strained, causing increases in bond length and bond angle disorder [20]. The G peak is sensitive mainly to the configuration of  $\text{sp}^2$  sites because of their higher cross-section, thus, the  $I_D/I_G$  ratio is a measure of the  $\text{sp}^2$  phase organized in rings [19]. The  $I_D/I_G$  ratio increases for both DLC and Si-DLC films with the inclusion of Si-C interlayer compared to the films without Si-C interlayer. From this it can be qualitatively asserted that the  $\text{sp}^2$  content increases while the  $\text{sp}^3$  content decreases as a result of the inclusion of the Si-C interlayer [21].

### 3.2. Adhesion

The adhesion levels for the DLC and Si-DLC films deposited on NBR were determined following the X-cut method described earlier. Fig. 5 shows optical microscopy images of X-cut locations after peel tests for the films. Table 1 was used to attribute adhesion levels for the DLC and Si-DLC films. From Fig. 6 it was observed that the DLC and Si-DLC films with Si-C interlayer had higher adhesion levels than the DLC and Si-DLC films without Si-C interlayer. For the DLC and Si-DLC films, jagged removal along incisions was observed up to 1.6 mm on either side of the X-cut resulting in an adhesion level of 3A. An adhesion level of 4A was determined for the films with Si-C interlayer due to trace peelings occurring along incisions with little peeling observed at the X-cut [16]. The good adhesion levels for all of the films may be attributed to the closed field unbalanced magnetron sputtering with ion plating system. This system enables plasma to be present in the deposition chamber between the target and the NBR substrate allowing energetic particles to bombard the substrate and enhance ionization of vapour species at even low energies. Particle bombardment of growing film surfaces causes densification of material and modified film properties [22]. A reduction of residual stresses can result from energetic ion bombardment of DLC films which improves film adhesion [23]. From the Raman spectroscopy results discussed for Fig. 4 it was seen that the inclusion of Si-C interlayer onto the DLC and Si-DLC films deposited on NBR substrates resulted in  $\text{sp}^2$  clusters becoming larger and less strained, leading to decreased bond length and bond angle

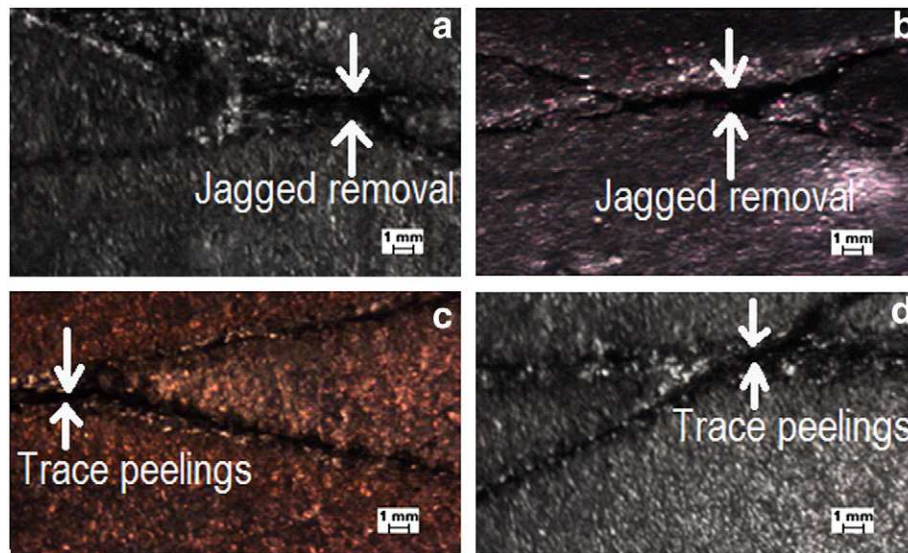


Fig. 5. Optical microscopy images of X-cut locations after peel tests for Si-DLC (a), DLC (b), DLC with Si-C interlayer (c) and Si-DLC with Si-C interlayer (d).

disorder, which results in a decrease in the magnitude of compressive residual stresses, and hence improving film adhesion [23].

### 3.3. Micro-hardness

Based on the geometry of the Vickers indenter, theoretical contact depth was calculated from the size of the diagonals, to help determine the relative influence of the substrate on the micro-hardness measurements. For indentations in coated systems these measurements reflect the properties of the coating only if the depth of indentation is less than one-tenth of the coating thickness [24]. Table 2 provides a summary of Vickers micro-hardness results for applied indentation loads of 147.1 mN, 490.3 mN and 981 mN, with calculated theoretical depth for DLC and Si-DLC films deposited on Si wafer.

For applied loads of 147.1 mN, the theoretical depth of the indentations did not exceed the film thickness for DLC and Si-DLC films without Si-C interlayer. However, as the depth was greater than one-tenth of the film thickness, the micro-hardness measurements were a function of both the coating and the substrate, thus, resulting in a composite micro-hardness measurement. At higher applied indentation loads of 490.3 mN and 981 mN, there is no statistical significance of the micro-hardness measurements. This is due to the fact that the penetration depth at these loads was much greater than the film thicknesses.

Fig. 6 shows the Vickers micro-hardness results for the films. It can be observed that the inclusion of the Si-C interlayer had distinct impacts on the hardness of the DLC and Si-DLC films. For the DLC film with Si-C

interlayer the hardness was 9.1 GPa, compared to 15.5 GPa for the DLC film without Si-C interlayer. This reduction in hardness is attributed to an increase in  $sp^2$  clusters which relieved the compressive stresses in the films. For the Si-DLC film with Si-C interlayer an average micro-hardness value of 12.1 GPa compared to 11.1 GPa for Si-DLC films was obtained. Fig. 7 shows the hardness of the films vs. the intensity ratio,  $I_D/I_G$ . A reduction in the film hardness corresponded to an increase in the intensity ratio for DLC, Si-DLC and DLC with Si-C interlayer films. This has earlier been explained qualitatively as resulting from an increase in  $sp^2$  content and a reduction in  $sp^3$  content [18,20]. However, for Si-DLC films with Si-C interlayer, contributions from  $sp^3$  sites due to vibrations of C–C  $sp^3$  bonds may be significant [17].

### 3.4. Tribology

The coefficient of friction as a function number of revolutions under an applied normal load of 5 N is shown in Fig. 8. The tribo-test showed a very interesting effect. All of the samples show a friction increase between 0.25 and 0.4 at 200 to 400 revolutions to between 0.45 and 0.6 at 4000 to 5000 revolutions indicating a clear transition region. As such, an analysis has been carried out to study the slope of the increase of the coefficient of friction as a function of number of revolutions (first derivative).

The frictional behaviour over the testing duration of 5000 revolutions was segmented into different regions for each coating: region AB, region BC and region CD. For each of these regions the slope was

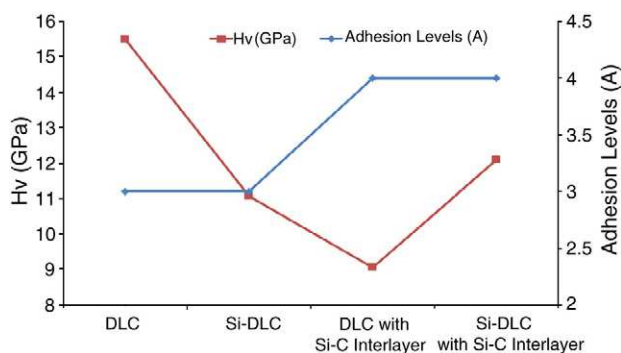
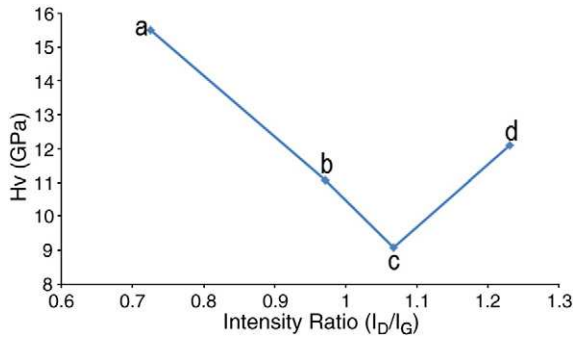


Fig. 6. Vickers hardness (at 147.1 mN indentation load) and adhesion levels for DLC and Si-DLC films without and with Si-C interlayer.

Table 2

Summary of Vickers micro-hardness (GPa) results for applied indentation loads of 147.1 mN, 490.3 mN, and 981 mN, with theoretical contact depth.

Coating	Applied force (mN)	d ( $\mu$ m)	Hv (average $\pm$ s.d)
DLC	147.1	0.6	15.5 $\pm$ 0.8
	490.3	1.3	10.5 $\pm$ 0.7
	981	1.9	9.4 $\pm$ 0.3
Si-DLC	147.1	0.7	11.1 $\pm$ 0.7
	490.3	1.4	9.7 $\pm$ 0.7
	981	2.0	8.6 $\pm$ 0.3
DLC with Si-C interlayer	147.1	0.8	9.1 $\pm$ 0.7
	490.3	1.4	9.6 $\pm$ 0.8
	981	2.1	8.4 $\pm$ 0.3
Si-DLC with Si-C interlayer	147.1	0.7	12.1 $\pm$ 1.2
	490.3	1.3	10.2 $\pm$ 0.3
	981	1.9	9.6 $\pm$ 0.4



**Fig. 7.** The micro-hardness (at 147.1 mN indentation load) of DLC (a), Si-DLC (b), DLC with Si-C interlayer (c) and Si-DLC with Si-C interlayer (d) films vs. intensity ratio,  $I_D/I_G$ .

determined as  $\Delta y/\Delta x$  (change in coefficient of friction/change in number of revolutions). The aim of determining this first derivative was so that an estimation of the film failure rate could be determined. Table 3 shows the results of the slope determinations for regions AB, BC and CD.

In the region AB, the highest slope was obtained for Si-DLC and DLC with Si-C interlayers, at  $22.5 \times 10^{-5}$  and  $8.6 \times 10^{-5}$ . The high slopes for DLC and Si-DLC films with Si-C interlayers in region AB can be related to the comparatively lower composite micro-hardness of these films at 9.1 GPa and 12.1 GPa, respectively. Si-DLC had a lower composite micro-hardness value of 11.1 GPa than Si-DLC with Si-C interlayer, but had a slope of  $5 \times 10^{-5}$ . This difference is explained by the inclusion of the Si-C interlayer that resulted in an increase in  $sp^2$  clusters that were unstrained and reduced compressive stress within the films. The lowest slope of  $2.3 \times 10^{-5}$  was obtained for DLC films. This is a direct result of the high composite micro-hardness values for these films at 15.5 GPa. Therefore, in region AB film failure classification from highest to lowest would be Si-DLC with Si-C interlayer, DLC with Si-C interlayer, Si-DLC and DLC films.

In region BC the lowest slope was obtained for Si-DLC with Si-C interlayer at  $1.3 \times 10^{-5}$ . This very low slope is an indicator that the film had stabilized at steady state conditions for the remainder of the tribo-test. However, for DLC, Si-DLC and DLC with Si-C interlayer the penetration of the pin deeper into the film/interlayer/substrate samples is related to the composite micro-hardness with higher slopes being observed for samples with lower composite hardness values. Therefore, low composite micro-hardness of films enhanced film failure in this region. In region CD, the slopes tend towards steady state conditions which may indicate that there was a transfer of the film onto the pin so that no more transitions are observed.

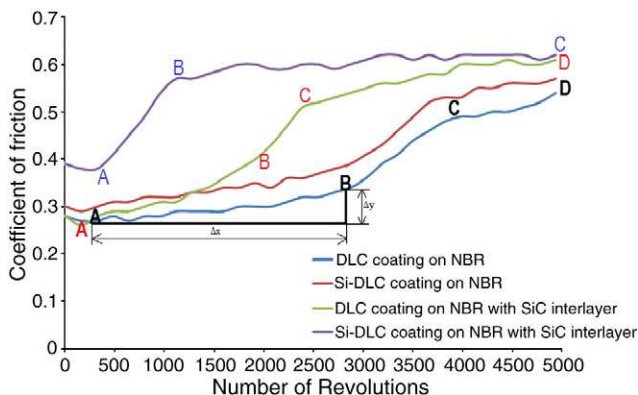


**Fig. 8.** Coefficient of friction vs. number of revolutions for DLC and Si-DLC with and without Si-C interlayer. Points A, B, C and D are indicated for estimation of slopes of the increase of the coefficient of friction.

**Table 3**

Slopes of coefficient of friction as a function of number of revolutions for DLC and Si-DLC films corresponding to regions AB, BC and CD for tribo-test under normal load of 5 N.

	Region AB ( $\times 10^{-5}$ )	Region BC ( $\times 10^{-5}$ )	Region CD ( $\times 10^{-5}$ )
DLC	2.3	11.4	4.6
Si-DLC	5.0	12.5	3.9
DLC with Si-C interlayer	8.6	25.0	3.8
Si-DLC with Si-C interlayer	22.5	1.3	–

In Fig. 9 the wear profiles for the wear tracks formed as a result of this tribo-test are shown. The wear profiles indicate non-uniformity of the wear tracks due to the visco-elastic behaviour of the NBR substrate. The highest average wear depth  $((W_1 + W_2)/2)$  was observed for Si-DLC and DLC with Si-C interlayer at 0.123 mm and 0.1 mm respectively. The lowest wear depth was measured for DLC and Si-DLC films at 0.068 mm and 0.073 mm respectively. This result can be explained by the higher micro-hardness value (15.5 GPa) for the DLC films. From the Raman spectroscopy analysis, it was determined that the inclusion of the Si-C interlayer results in an increase in  $sp^2$  clusters, which relieve compressive residual stresses, as such DLC and Si-DLC films with Si-C interlayers have lower composite micro-hardness, with corresponding higher wear depth compared to DLC and Si-DLC films without Si-C interlayer. The higher wear depth of Si-DLC films is attributed to doping with Si [25]. According to Archard's wear law [26], wear rate or volume is inversely proportional to hardness. Therefore as wear depth increases the film composite micro-hardness is expected to reduce as the pin transits from contact between the DLC/Si-DLC top layer, to the Si-C interlayer to the NBR substrate or between DLC/Si-DLC top to the NBR substrate. Due to influence of the substrate viscoelasticity, the wear depth increases in each pass of the ball over the film, with less wear expected for films with higher micro-hardness. However, once film failure occurs, overall wear depth increases rapidly before reaching a steady state [27].

#### 4. Conclusion

The deposited coatings showed excellent adherence with an adhesion rating of 4 A for films with a Si-C interlayer. The composite micro-hardness was highest for DLC films at 15.5 GPa for an indentation load of 147.1 mN using a Vickers micro-hardness tester. The adhesion and micro-hardness behaviour were related to the hybridization of carbon in terms of  $sp^2$  and  $sp^3$  bonding. Tribological tests undertaken under normal load of 5 N using a pin-on-disc tribometer for all of the samples of DLC and Si-DLC films, with and without Si-C interlayer show a friction increase between 0.25 and 0.4 to between 0.45 and 0.6. It has been shown that the friction increase in region AB is determined by the combined effect of the inclusion of the Si-C interlayer and the composite micro-hardness. Film failure classification from highest to lowest was determined as Si-DLC with Si-C interlayer, DLC with Si-C interlayer, Si-DLC and DLC films. In region BC, the friction increase is due to only the micro-hardness effects for DLC, Si-DLC films and DLC films with Si-C interlayer. These results indicate that the application of DLC and Si-DLC films with and without Si-C interlayers onto actual piston seals may be advantageous.

#### Acknowledgements

The authors would like to acknowledge the financial support provided by the Water is Life project under Irish Aid and Higher Education Authority partnership of the Republic of Ireland for the financial support to carry out the research.

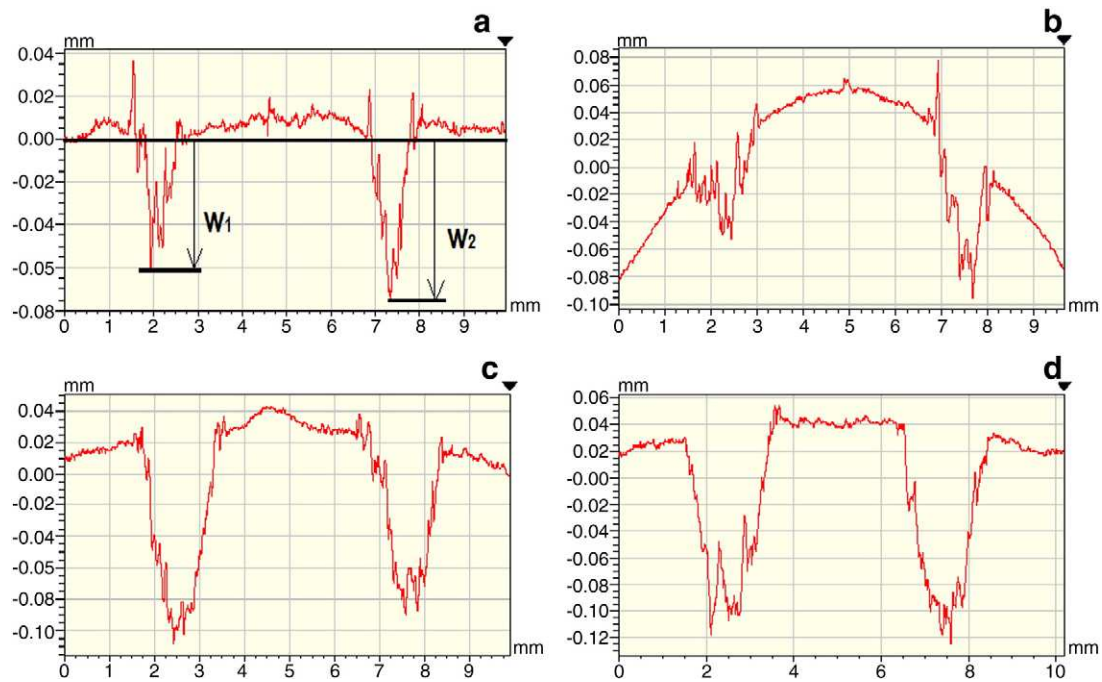


Fig. 9. Wear profile of the wear tracks for the films under a load of 5 N. DLC – a; Si-DLC – b; DLC with Si-C interlayer – c; Si-DLC with Si-C interlayer – d.

## References

- [1] L. Martinez, R. Nevshupa, L. Alvarez, Y. Huttel, J. Mendez, E. Roman, E. Mozas, J.R. Valdes, M.A. Jimenez, Y. Gachon, C. Heau, F. Faverjon, *Tribol. Int.* 42 (2009) 584.
- [2] Y.T. Pei, X.L. Bui, J.Th.M. De Hosson, *Thin Solid Films* 518 (2010) 552.
- [3] X.L. Bui, Y.T. Pei, J.Th.M. De Hosson, *Surf. Coat. Technol.* 202 (2008) 4939.
- [4] D. Martinez-Martinez, M. Schenkel, Y.T. Pei, J.C. Sanchez-Lopez, J.Th.M. De Hosson, *Surf. Coat. Technol.* 205 (2011) S75.
- [5] Y.T. Pei, X.L. Bui, X.B. Zhou, J.Th.M. De Hosson, *Surf. Coat. Technol.* 202 (2008) 1869.
- [6] X.L. Bui, Y.T. Pei, E.D.G. Mulder, J.Th.M. De Hosson, *Surf. Coat. Technol.* 203 (2009) 1964.
- [7] M. Lubwama, K.A. McDonnell, J.B. Kirabira, A. Sebbit, K. Sayers, D. Dowling, B. Corcoran, *Surf. Coat. Technol.* (2012), <http://dx.doi.org/10.1016/j.surfcoat.2012.05.015>.
- [8] Q.R. Hou, J. Gao, S.J. Li, *Eur. Phys. J. B* 8 (1999) 493.
- [9] B. Ollivier, A. Matthews, *J. Adhes. Sci. Technol.* 8 (6) (1994) 651.
- [10] G.D. Vaughn, B.G. Frushour, W.C. Dale, *J. Adhes. Sci. Technol.* 8 (6) (1994) 635.
- [11] M.J. Freeman, D.R. Harding, *J. Polym. Sci. B* 32 (1994) 1377.
- [12] J. Lankford, C.R. Blanchard, C.M. Agrawal, D.M. Micallef, G. Dearnaley, A.R. McCabe, *Nucl. Instrum. Methods* 80 (1993) 1441.
- [13] Y.-B. Guo, F.C.-N. Hong, *Diamond Relat. Mater.* 12 (2003) 946.
- [14] I.Sh. Trakhtenberg, O.M. Bakunin, I.N. Korneyev, S.A. Plotnikov, A.P. Rubshtein, K. Uemura, *Diamond Relat. Mater.* 9 (2000) 711.
- [15] P.M. Martin, *Handbook of deposition technologies for films and coatings*, 2009, p. 23.
- [16] American Society for Testing and Materials, Designation: D-3359-97, *Standard Test Methods for Measuring Adhesion by Tape Test* (1998) 368.
- [17] K.W.R. Gilkes, S. Praver, K.W. Nugent, J. Robertson, H.S. Sands, Y. Lifshitz, X. Shi, *J. Appl. Phys.* 87 (2000) 7283.
- [18] N. Paik, *Surf. Coat. Technol.* 200 (2005) 2170.
- [19] R. Paul, S.N. Das, S. Dalui, R.N. Gayen, R.K. Roy, R. Bhar, A.K. Pal, *J. Phys. D: Appl. Phys.* 41 (2008) 055309.
- [20] C. Casiraghi, A.C. Ferrari, J. Robertson, *Phys. Rev. B* 72 (2005) 085401.
- [21] A.C. Ferrari, J. Robertson, *Phys. Rev. B* 61 (2000) 14095.
- [22] U. Helmersson, M. Lattemann, J. Bohlmark, A.P. Ehiastian, J.T. Gudmundsson, *Thin Solid Films* 513 (2006) 1.
- [23] Y. Pauleau, in: C. Donnet, A. Erdemir (Eds.), *Tribology of diamond-like carbon films*, Springer, 2008, p. 102.
- [24] S.V. Hainsworth, T.F. Page, *Mater. Res. Soc. Symp. Proc.* 436 (1997) 171.
- [25] P. Papakonstantinou, J.F. Zhao, P. Lemoine, E.T. McAdams, J.A. McLaughlin, *Diamond Relat. Mater.* 11 (2004) 1074.
- [26] J.F. Archard, *J. Appl. Phys.* 24 (1953) 981.
- [27] D. Martinez-Martinez, J.P. van der Pal, Y.T. Pei, J.Th.M. De Hosson, *J. Appl. Phys.* 110 (2011) 124906.